THE JOURNAL OF BIOLOGICAL CHEMISTRY VOL. 284, NO. 29, pp. 19392–19401, July 17, 2009

Docking of PRAK/MK5 to the Atypical MAPKs ERK3 and ERK4 Defines a Novel MAPK Interaction Motif*

Received for publication, March 16, 2009, and in revised form, May 20, 2009 Published, JBC Papers in Press, May 27, 2009, DOI 10.1074/jbc.M109.023283

Espen Åberg[‡], Knut Martin Torgersen[§], Bjarne Johansen[¶], Stephen M. Keyse[‖], Maria Perander[¶], and Ole-Morten Seternes[‡1]

From the Institutes of [‡]Pharmacy and [¶]Medical Biology, University of Tromsø, N-9037 Tromsø, Norway, the [§]Biotechnology Centre of Oslo, University of Oslo, N-0317 Oslo, Norway, and [‖]Cancer Research UK Stress Response Laboratory, Biomedical Research Institute, Ninewells Hospital and Medical School, Dundee DD1 9SY, Scotland, United Kingdom

ERK3 and ERK4 are atypical MAPKs in which the canonical T*X*Y motif within the activation loop of the classical MAPKs is replaced by SEG. Both ERK3 and ERK4 bind, translocate, and activate the MAPK-activated protein kinase (MK) 5. The classical MAPKs ERK1/2 and p38 interact with downstream MKs (RSK1–3 and MK2–3, respectively) through conserved clusters of acidic amino acids, which constitute the common docking (CD) domain. In contrast to the classical MAPKs, the interaction between ERK3/4 and MK5 is strictly dependent on phosphorylation of the SEG motif of these kinases. Here we report that the conserved CD domain is dispensable for the interaction of ERK3 and ERK4 with MK5. Using peptide overlay assays, we have defined a novel MK5 interaction motif (FRIEDE) within both ERK4 and ERK3 that is essential for binding to the C-terminal region of MK5. This motif is located within the L16 extension lying C-terminal to the CD domain in ERK3 and ERK4 and a single isoleucine to lysine substitution in FRIEDE totally abrogates binding, activation, and translocation of MK5 by both ERK3 and ERK4. These findings are the first to demonstrate binding of a physiological substrate via this region of the L16 loop in a MAPK. Furthermore, the link between activation loop phosphorylation and accessibility of the FRIEDE interaction motif suggests a switch mechanism for these atypical MAPKs in which the phosphorylation status of the activation loop regulates the ability of both ERK3 and ERK4 to bind to a downstream effector.

Mitogen-activated protein kinase (MAPK)[2] phosphorylation cascades play important roles in the regulation of diverse cellular functions such as cell proliferation, differentiation, migration, and apoptosis (1, 2). A characteristic and conserved feature of this family of signaling pathways is their organization into modules comprising a sequential three-tiered kinase cascade. This contains a MAPK kinase kinase, a MEK, and the MAPK itself. Four such MAPK signaling modules have been described in mammals: ERK1 and ERK2, the c-Jun N-terminal kinases 1–3, the p38 kinases (p38$\alpha/\beta/\gamma/\delta$), and ERK5 (3–7). The MAPK kinase kinases phosphorylate and activate the MEKs, which in turn activate the MAPKs by dual phosphorylation on both the threonine and the tyrosine residue of a highly conserved T*X*Y motif in the kinase activation loop. MAPKs are Ser/Thr kinases, which phosphorylate a wide range of substrates with the minimal consensus sequence (S/T)P (2).

ERK4 and its close relative ERK3 are regarded as atypical members of the MAPK family. In contrast to the classical MAPKs, ERK3 and ERK4 harbor an SEG motif in the activation loop and thus lack a second phosphoacceptor site. In addition, protein kinases all possess a conserved APE motif located just C-terminal to the phosphoacceptor sites within subdomain VIII, in which the conserved glutamate is important for maintaining the stability of the kinase domain. In both ERK3 and ERK4, this motif is substituted by SPR, and ERK3 and ERK4 are the only two protein kinases in the human genome with an arginine residue in this position (8). Although they display significant sequence homology (44% identity) with ERK1 and ERK2 within their kinase domains, both ERK3 and ERK4 have unique C-terminal extensions, which account for the large differences in size observed between ERK1/2 (~360 amino acids) and ERK3/ERK4 (721/587 amino acids). Whereas classical MAPKs have been highly conserved throughout evolution, with examples found in both unicellular and multicellular organisms, ERK3 and ERK4 are only present in vertebrates. Finally, in contrast to many of the classical MAPKs, the regulation, substrate specificity, and physiological functions of ERK3 and ERK4 are poorly understood. Although ERK3 and ERK4 are very similar to each other, there are significant differences between them. For instance, whereas ERK4, like most classical MAPKs, is a stable protein, ERK3 is highly unstable and subject to rapid proteosomal degradation. Thus, ERK3 activity may be regulated at the level of cellular abundance, and taken together these features indicate that ERK3 and ERK4 may perform specialized functions and enjoy different modes of regulation when compared with classical MAPKs (9–11).

Despite the striking differences between ERK3 and ERK4 and the classical MAPKs, they do share one property with the ERK1/2, p38, and ERK5, namely the ability to interact with a group of downstream Ser/Thr protein kinases, termed MAPK-activated protein kinases (MAPKAPKs or MKs) (12, 13). In the

* This work was supported by the National Programme for Research in Functional Genomics in Norway of the Research Council of Norway, the Norwegian Cancer Society, the Blix Family Foundation, and a Cancer Research UK Programme grant (to S. M. K.).

[1] Fellow of the Norwegian Cancer Society. To whom correspondence should be addressed. Tel.: 47-77-64-65-06; Fax: 47-77-64-61-51; E-mail: ole-morten.seternes@uit.no.

[2] The abbreviations used are: MAPK, mitogen-activated protein kinase; CD, common docking; ERK, extracellular signal-regulated kinase; MEK, MAPK/ERK kinase; MK or MAPKAPK, MAPK-activated protein kinases; GFP, green fluorescent protein; GST, glutathione *S*-transferase; WT, wild type; CDm, CD mutant; EGFP, enhanced GFP.

case of ERK3 and ERK4, both proteins interact with, translocate, and activate the MK5 protein kinase. Several studies have drawn attention to the role of specific docking interactions that contribute to both substrate selectivity and regulation in MAPK pathways (14–17). These interactions involve docking domains, which specifically recognize small peptide docking motifs (D motifs) located on functional MAPK partner proteins including downstream substrates, scaffold proteins, as well as positive and negative regulators. The docking domains, although located within the kinase domains, are distinct from the active site. Similarly the D motifs, which these docking domains recognize, are also distinct from the phosphoacceptor sites within protein substrates (18). There are several classes of D motifs. The motifs found in MAPKAP kinases including MK5 have the consensus sequence $LX_{1-2}(K/R)_{2-5}$ where X is any amino acid (12). The corresponding docking domains within the MAPKs have also been characterized (16, 19, 20). The common docking (CD) domain is a cluster of negatively charged amino acids located in the L16 extension directly C-terminal to the kinase domain in the MAPK primary structure. A second domain termed ED (Glu-Asp) also contributes to binding specificity. This latter site is located near the CD domain in the MAPK tertiary structure. Whereas the CD domain is considered commonly important for all docking interactions, the ED site is thought to be important for the determination of specificity (16). Other residues and regions distinct from the ED and CD domains have also been shown to be important for docking.(21–25).

This work has so far been largely confined to analysis of the classical MAPKs, and much less is known about the nature of substrate or regulatory docking interactions for the atypical MAPKs. We and others (9, 11, 26) have recently reported that the region encompassing residues 326–340 within both ERK3 and ERK4 is required for their ability to interact with and activate MK5. Furthermore, a truncated mutant of MK5, which lacks the 50 C-terminal residues (MK5 1–423), was unable to bind to ERK4 despite the fact that it retains its D domain. Finally, in contrast to conventional MAPKs, the interaction between ERK3 and ERK4 and MK5 requires activation loop phosphorylation of ERK3 and ERK4 (27, 28). Taken together these observations suggest that the mechanism by which the atypical MAPKs recognize and bind to at least one important class of effector kinases may be distinct to that found in the classical MAPKs such as ERK1/2 and p38.

Here we demonstrate that two separate C-terminal regions, encompassing residues 383–393 and 460–465, respectively, are necessary for MK5 to interact with both ERK3 and ERK4. These regions are distinct from the D motif previously identified within MK5, suggesting that binding to ERK3 and ERK4 may be mediated by a different mechanism to that seen in the classical MAPKs. In support of this, the conserved CD domains within ERK3 and ERK4 are shown to be completely dispensable for MK5 interaction. Using peptide overlay assays, we have defined a minimal MK5 interaction motif FRIEDE in ERK4. Furthermore, we demonstrate that a single point mutation (ERK3 I334K or ERK4 I330K) within this FRIEDE motif is sufficient to disrupt the binding of both ERK3 and ERK4 to MK5 and consequently their ability to both translocate and activate MK5. The FRIEDE motif is located within the L16 extension C-terminal to the CD domain in both ERK3 and ERK4. Interestingly, molecular modeling of the corresponding region in ERK2 suggests that it undergoes a significant conformational change as a result of activation loop phosphorylation, making this part of the L16 extension more accessible (29). We propose that the FRIEDE motif represents a novel MAPK interaction motif, the function of which is linked to activation loop phosphorylation and MAPK activation.

EXPERIMENTAL PROCEDURES

Reagents—Bovine serum albumin and cycloheximide were purchased from Sigma-Aldrich.

Antibodies—A sheep polyclonal anti-ERK4 antibody and an anti-PRAK Thr(P)^{182} antibody were kindly provided by Prof. P. Cohen (Medical Research Council Protein Phosphorylation Unit, University of Dundee, Dundee, UK). Alexa Fluor 680 goat anti-rabbit IgG (A21076), Alexa Fluor 680 goat anti-mouse IgG (A-21057), Alexa Fluor 594 goat anti-mouse (A11020), and Alexa Fluor 680 donkey anti-sheep IgG (A-21102) were purchased from Molecular Probes, Inc. (Eugene, OR). IRDye 800CW-conjugated affinity-purified anti-mouse IgG (610-131-121), IRDye 800CW-conjugated affinity-purified anti-rabbit IgG (611-131-122), and conjugated anti-GFP IRDye 800-conjugated GFP antibody (600-132-215) were acquired from Rockland Immunochemicals (Gilbertsville, PA). The monoclonal Myc9E10 and anti-MK5 A7 (sc-46667) antibodies were purchased from Santa Cruz Biotech (Santa Cruz, CA). EZview Red anti-c-Myc affinity gel (E6654) was obtained from Sigma-Aldrich. The rabbit polyclonal anti-GFP antibody was kindly provided by T. Johansen (University of Tromsoe).

Cell Culture and Transfection—HeLa cells were maintained in Eagle's minimum essential medium supplemented with 1× nonessential amino acids (Invitrogen), 10% fetal bovine serum (Invitrogen), 2 mM L-glutamine, penicillin (100 units/ml), and streptomycin (100 μg/ml). Lipofectamine Plus (Invitrogen) reagent was used to transfect the HeLa cells according to the manufacturer's instructions.

Cell Staining and Microscopy—Determination of the subcellular localization of GFP fusion proteins, Myc-tagged ERK3, and ERK4 and the visualization of cell nuclei was performed as described previously (11). The images were collected using a Zeiss LSM510 confocal laser-scanning microscope and processed using Adobe Photoshop.

DNA Constructs—Construction of pENTR-D-ERK4, pEXPmycERK4wt (Myc-ERK4-WT) (9), and pSGERK3-Myc (Myc-ERK3-WT) has been described previously. The pENTR-D-MK5 was generated by PCR amplification of the open reading frame of murine MK5 and subsequent cloning into pENTR-D-TOPO (Invitrogen). The following plasmids were constructed by mutagenesis of either pENTR-D-ERK4 or pENTR-D-MK5 using the QuikChange site-directed mutagenesis kit (Stratagene) and subsequent recombination into the Gateway destination vectors pDESTmyc or pDESTEGFP (30): pmycERK4CDmut, pmycERK4F328A, pmycERK4F328Y, pmycERK4 I330K, pmycERK4 F328A,I330K, and pEGFP-MK5. Expression constructs for deletion mutants of MK5 were made by PCR amplification and cloning into pENTR-D-TOPO

before recombination into the gateway destination vectors pDESTEGFP to generate pEXPEGFP-MK5 350–473, pEGFP 372–473, pEGFP-MK5 383–473, pEGFP-MK5 393–473, pEGFP-MK5 1–465, and pEXPEGFP-MK5 1–460. QuikChange site-directed mutagenesis kit were used to generate mycERK3F332A, mycERK3F332Y, and mycERK3I334K with pSGERK3-Myc as template. Details on their construction are available upon request. All of the plasmid constructs described were verified by DNA sequencing using the BigDye Terminator v3.1 cycle sequencing kit (Applied Biosystems). All of the PCRs were performed using Pfx platinum polymerase (Invitrogen) according to the manufacturer's instructions.

Immunoblotting—For detection of epitope-tagged ERK3, ERK4, and MK5 in transfected cells and co-immunoprecipitation experiments, the samples were analyzed by SDS-PAGE (4–12% NUPAGE; Invitrogen), transferred to a nitrocellulose membrane (Amersham Biosciences), and probed with either anti-Myc (1:200, 9E10; Santa Cruz), anti-HA (1:1000; 12CA5; Roche Applied Science), anti-ERK4 (1:1000), anti-P-T182-MK5 (1:500), anti-MK5 (1:500, A7, Santa Cruz), or anti-GFP IRDye^{TM} 800-conjugated (1:5000; Rockland Inc). Detection and quantification were performed either directly with anti-GFP IRDye^{TM} 800-conjugated antibody or by conjugated goat anti-mouse IgG (H&L) or IRDye 800CW-conjugated goat anti-rabbit IgG (H&L) (1:5000; Rockland Inc.) or Alexa Fluor 680-conjugated donkey anti-sheep IgG (H&L) (1:5000; Molecular Probes, Inc.) and the Odyssey Infrared Imaging System (Li-Cor Biosciences). The molecular weights were estimated using the MagicMark Western protein standard (Invitrogen).

Expression of GST Fusion Proteins in Escherichia coli—GST-MK5 fusion protein was expressed in *E. coli* (BL21) and purified as previously described. SDS-PAGE and Coomassie Blue staining were used to analyze both the expression and yield of the fusion proteins.

SPOT Synthesis of Peptide Arrays and GST Overlay Assay—Peptide arrays were synthesized on cellulose membranes using a MultiPep automated peptide synthesizer (INTAVIS Bioanalytical Instruments AG, Germany) as described (31). The filters were blocked in TBS-T with 5% milk and peptide interactions with GST and GST-MK5 fusion proteins were determined by overlaying the cellulose membranes with 1 μg/ml of protein for 2 h at room temperature. After washing in TBS-T, the bound proteins were detected with horseradish peroxidase-conjugated anti-GST antibodies (1:5000, clone RPN1236; GE/Amersham Biosciences).

Molecular Modeling—The illustration of the (hypothetical) model of the "ERK4 Ile^{330} flip" was generated using swiss-PDB viewer (32) and PyMol using inactive and active conformations of ERK2 (Protein Data Bank accession numbers 1ERK and 2ERK, respectively) as templates.

RESULTS

Multiple Determinants within the C Terminus of MK5 Mediate Its Interaction with ERK4—We and others (9, 26, 33) have recently identified ERK4 as a *bona fide* interaction partner for MK5. Upon binding to ERK4, MK5 is phosphorylated and activated, and complex formation also promotes the relocalization of MK5 from the nucleus to the cytoplasm. The C-terminal 50 amino acids of MK5 are essential for this interaction, because a C-terminal truncation mutant comprising residues 1–423 of MK5 is unable to bind to ERK4 (9). To further dissect the domain(s) within MK5 that are responsible for its interaction with ERK4, a series of EGFP-tagged C- and N-terminal MK5 deletion mutants were constructed (Fig. 1*A*). To dissect out the minimal ERK4-binding domain, we first co-expressed the N-terminal MK5 deletion mutants with ERK4 in HeLa cells and performed co-immunoprecipitations to assess binding activity. Our results clearly show that residues 383–473 of MK5 are sufficient for both ERK3 and ERK4 binding. In contrast, the deletion of another 11 residues from the N terminus of this protein abrogated its ability to bind to ERK3 and ERK4 (Fig. 1, *B* and *C*). Next, the EGFP-MK5 C-terminal deletion mutants were co-expressed with either full-length Myc-tagged ERK3 or ERK4 in HeLa cells. Immunoprecipitation of EGFP-MK5 followed by immunoblotting for ERK3 or ERK4 revealed that loss of the last 13 amino acids of MK5 (MK5 1–460) completely abrogated interaction with both ERK3 and ERK4 (Fig. 1, *D* and *E*). In contrast, loss of only 8 residues from the C terminus of MK5 (MK5 1–465) did not affect the ability of MK5 to bind to ERK3 or ERK4 (Fig. 1, *D* and *E*). Like WT MK5, both of these C-terminal truncation mutants are localized in the cell nucleus when expressed as EGFP fusion proteins (Fig. 1, *F* and *G*). As expected, co-expression of ERK4 with either wild type MK5 or the C-terminal deletion of MK5 protein lacking only 8 residues leads to relocalization of these MK5 proteins from nucleus to cytoplasm (Fig. 1, *G* and *F*). In contrast, the C-terminal deletion mutant of MK5 lacking 13 residues is not completely relocalized on co-expression of ERK5 with staining observed in both nucleus and cytoplasm (Fig. 1, *G* and *F*). Taken together, our data strongly suggest that regions encompassing residues 383–393 and 460–465 of MK5 contribute to ERK3 and ERK4 binding.

Neither the CD Domain nor the Glu-Asp (ED) Domain within ERK4 Mediates Its Interaction with MK5—Previous studies have identified the CD and ED domains of MAPKs as important for interaction with various binding partners (19, 20). The CD domain is a cluster of negatively charged amino acids located in the L16 extension directly C-terminal to the kinase domain in the MAPK primary structure. Although this domain is present in all MAPKs, nothing is known about docking determinants within the ERK3/4 subgroup. By homology with other MAPKs, the ERK3 and ERK4 CD domains lie between residues 316–330 and 312–326, respectively (Fig. 2*A*). The ED domains were also conserved, lying between residues 160 and 167 in ERK3 and residues 157 and 163 in ERK4. To test the function of these two domains with respect to interactions with MK5, we generated ERK4 constructs carrying point mutations in core residues within both the CD and ED motifs. The ERK4 CD mutant (CDm) was generated by substitution of Glu^{319} with Gln and Asp^{320} with Asn. The Aspartic acid substitution is analogous to the *sevenmaker* gain-of-function mutant found in the *Drosophila* ERK/rolled MAPK (34), whereas Glu^{319} has also been implicated in CD domain function (20). Recently, two distinct C-terminal ERK4 deletion mutants, ERK4 1–325 (9, 26) and ERK4 1–330 (9, 26) were shown to be unable to mediate both binding to MK5 and its translocation from the nucleus to the cytoplasm.

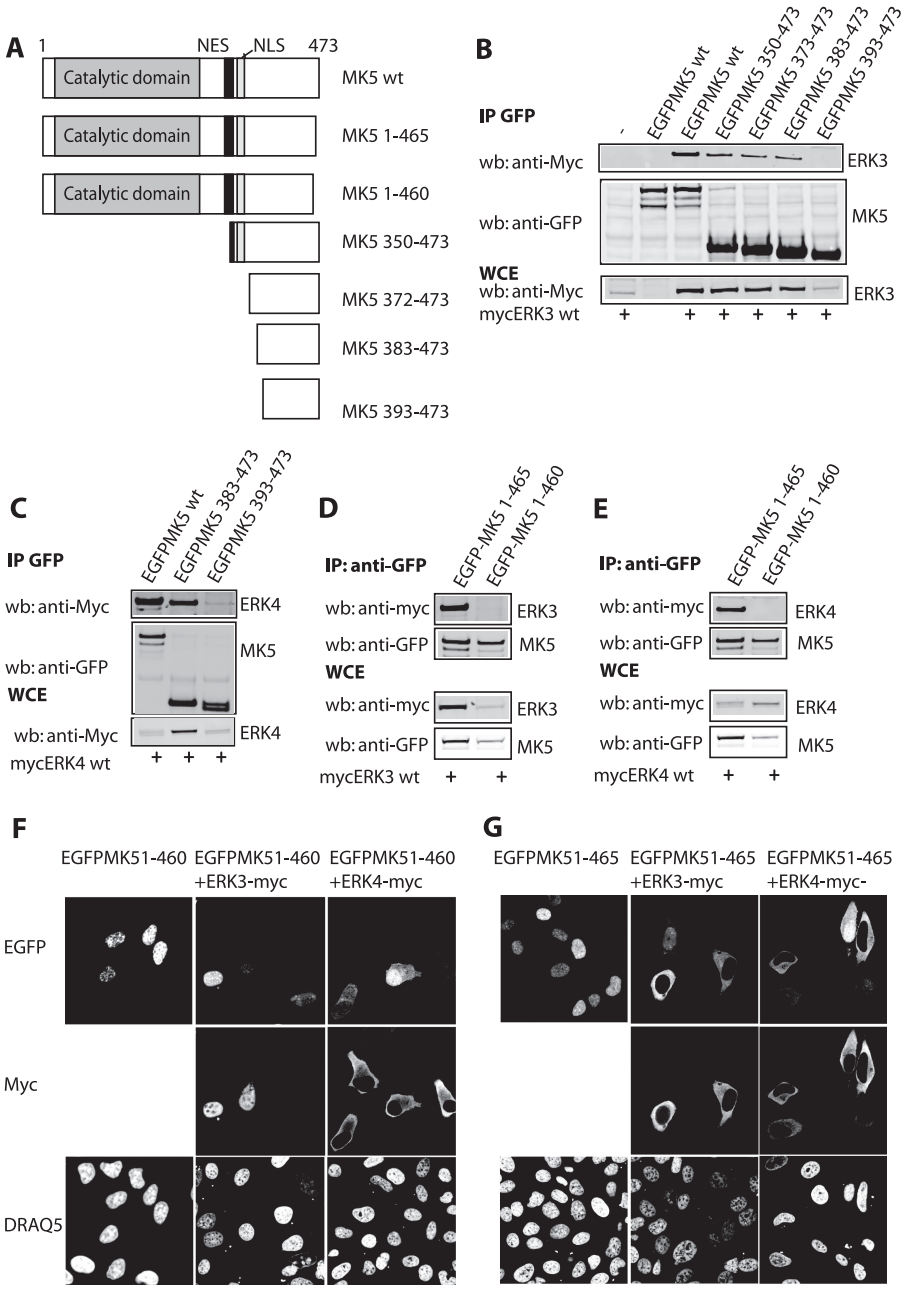

FIGURE 1. **Multiple determinants within the C terminus of MK5 are important for interaction with ERK4.** *A*, schematic representation of the MK5 constructs used is shown. *B* and *C*, EGFP co-immunoprecipitation (*IP*) assays were performed on lysates from HeLa cells co-transfected with the indicated expression vectors. Bound ERK3 (*B*) or ERK4 (*C*) was detected using an anti-Myc antibody (*top panel*). EGFPMK5 was detected with an anti-GFP antibody (*middle panel*). Equal expression of ERK3 and ERK4 was verified by Western blotting (*wb*) of the whole cell extract (*WCE*) with anti-Myc antibody (*bottom panel*). *D* and *E*, HeLa cells were co-transfected with vectors encoding either Myc-ERK3 (*D*) or Myc-ERK4 (*E*) and EGFP-MK5 1–465 or EGFP-MK5 1–460. After 24 h, whole cell extracts were prepared and ERK4 was immunoprecipitated with an anti-GFP antibody. Co-immunoprecipitated ERK3 (*D*) or ERK4 (*E*) was detected by Western blot analysis using an anti-Myc antibody (*top panel*), whereas MK5 was detected using a polyclonal anti-GFP antibody (*second panel*). Equal expression of ERK3 and ERK4 or EGFP-MK5 were verified by Western blotting of the whole cell extract with anti-Myc antibody (*third panel*) or anti-GFP antibody (*bottom panel*). *F* and *G*, HeLa cells were co-transfected with expression vectors encoding EGFP-MK5 1–460 or EGFP-MK5 1–465 and mycERK3 (*F*) or Myc-ERK4 (*G*). After 24 h, the cells were fixed, and EGFP-MK5 was visualized directly (*top panel*), and ERK3 or ERK4 was visualized by staining with an anti-Myc antibody and an Alexa 594-coupled secondary (anti-mouse) antibody (*middle panel*). The cell nuclei were visualized by DRAQ5 staining (*bottom panel*).

Interestingly, both of these deletion mutants still contain the CD motif. This suggests that the CD domain alone is not sufficient for MK5-ERK4 complex formation. In agreement with these results, we also found that ERK4 CDm interacted strongly with MK5 in our co-immunoprecipitation assays (Fig. 2*B*), and this mutant also relocalized MK5 to the cytoplasm of HeLa cells as efficiently as the wild type protein (Fig. 2*C*). We also examined the function of the ERK4 ED domain by expressing an ERK4 mutant in which both the CD domain and the ED site were mutated (CDEDm: E160T,D161T), but these additional substitutions had no effect on the ability of ERK4 to co-immunoprecipitate MK5 (Fig. 2*B*). Point mutations within the core CD domain of ERK3 also had no effect on its ability to interact with MK5 (data not shown). We conclude that key conserved residues within both the CD and ED domains of both ERK3 and ERK4 are not essential for docking interactions with MK5.

Identification of a Novel Motif (FRIEDE) within ERK4 as Essential for Binding to MK5—Previous work has shown that although ERK4 1–325 does not bind to MK5, ERK3 1–340 and ERK4 1–340, which include a slightly larger part of the L16 loop, retain MK5 binding. These data implicate the 15-residue region lying immediately C-terminal to the ERK3 and ERK4 CD domains in the interaction with MK5 (9, 26). Fig. 3*E* presents a primary sequence alignment of various MAPKs over the region corresponding to residues 326–340 of ERK4. To characterize the binding of MK5 to this region at high resolution, we performed a peptide walk through amino acids 292–370 of ERK4 by synthesizing a SPOT peptide array on cellulose membranes consisting of 20-mer peptides at 1-amino acid intervals. This array was probed with either purified recombinant GST or GST-MK5 fusion proteins, and interactions were detected with an anti-GST antibody conjugated to horseradish peroxidase. In agreement with the previous results, this method confirmed the binding of MK5 to ERK4 in a region C-terminal to the CD domain. As shown in Fig. 3*A*, GST-MK5 specifically interacted with a series of peptides corresponding to amino acids 314–347 of ERK4 (highlighted sequence). Overlay with GST alone gave virtually no signal,

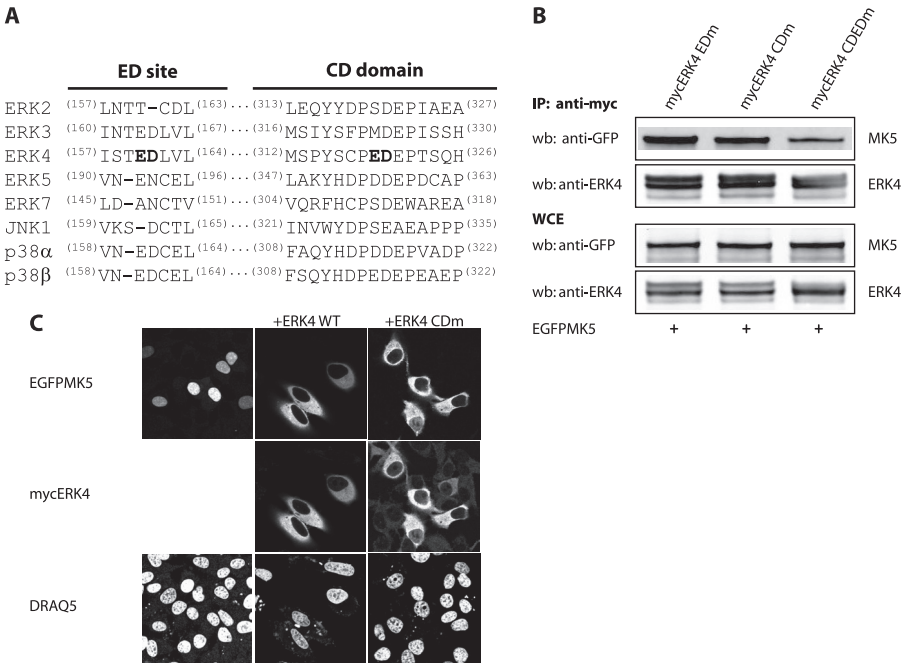

FIGURE 2. **The CD domain of ERK4 is dispensable for its ability to interact with MK5.** *A*, amino acid sequences in the CD domains for different human members of the MAPK family are shown. Residues in *bold type* indicate surface-exposed and negatively charged amino acids within the CD domain that are close to one another in the tertiary structure (20). *Bold type* indicate mutations introduced by us within the ERK4 CD domain (ERK4 CDm) and ED site (ERK4 CDEDm). *B*, HeLa cells were co-transfected with EGFP-MK5 and Myc-ERK4 WT, Myc-ERK4 CDm, or Myc-ERK4 CDEDm. After 24 h, the cells were lysed, and Myc-ERK4 was immunoprecipitated (*IP*) using an anti-Myc antibody. The immunoprecipitates were then analyzed by SDS-PAGE and Western blotting (*wb*) using either an anti-GFP antibody against MK5 (*top panel*) or an anti-ERK4 antibody (*second panel*). Equal expression of EGFP-MK5 and ERK4 were verified by Western blotting of the whole cell extract (*WCE*) with either an anti-GFP antibody (*third panel*) or anti-Myc antibody (*bottom panel*). *C*, HeLa cells were co-transfected with Myc-ERK4 WT or Myc-ERK4 CDm. After 24 h, the cells were fixed, and EGFP-MK5 was visualized directly (*top panel*), and ERK4 was visualized by staining with an anti-Myc antibody and an Alexa 594-coupled secondary (anti-mouse) antibody (*middle panel*). The cell nuclei were visualized by DRAQ5 staining (*bottom panel*).

indicating that these interactions are MK5-specific. To further define the boundaries of this interaction, peptides with N- and C-terminal deletions were spotted and probed with GST-MK5 (Fig. 3*B*). These systematic truncations revealed Phe^{328} and Glu^{333} as boundaries for MK5 binding and suggest a core binding motif defined by the sequence FRIEDE. The essential role of this sequence was supported in a systematic alanine scan in which point mutations identified Phe^{328} and Ile^{330} in the FRIEDE motif as critical for MK5 binding (Fig. 3*C*). Using these data we selected an 18-mer peptide, EPTSQHPFRIEDEIDDIV, corresponding to residues 321–338 of ERK4, for a two-dimensional peptide array screen in which every residue of the ERK4 sequence was substituted by each of the 19 other amino acids. Probing these 396 peptides with GST-MK5 confirmed the critical importance of Phe^{328} (Fig. 3*D*, *left panel*). Nearly all of the substitutions made at this position effectively disrupted the interaction with only amino acids carrying aromatic side groups (Tyr or Trp) able to substitute for the phenylalanine at this position. Another result from this screen was that individual lysine substitutions of residues His^{326} through Val^{338} resulted in significantly reduced affinity for MK5. Interestingly, substitution of phenylalanine into several positions seemed to stabilize the interaction. Based on sequence similarity and the ability to bind MK5, we performed a parallel experiment assaying the homologous region in ERK3. Two-dimensional array of the ERK3 sequence ^{325}EPISSHPFHIEDEVDDIL^{342} provided almost identical results to those obtained for ERK4 (Fig. 3*D*, *right panel*), indicating that similar determinants exist for MK5 binding by both proteins.

Together these data clearly suggest that ERK3 and ERK4 can effectively bind to MK5 independently of the CD domain and that key residues within the L16 extension generate a core interaction surface essential for this binding. To further verify the selectivity of MK5 for the FRIEDE motif in ERK3 and ERK4, we arrayed the corresponding sequences of 13 different human MAPKs, plus Hog1, the p38 MAPK homologue of *Saccharomyces cerevisiae* (scHog1) and *Drosophila* ERK (dmERK) on a filter and probed with GST-MK5 (Fig. 3*F*). Confirming the specificity of this interaction, MK5 bound strongly to ERK3 and ERK4 with only a weak interaction observed for ERK5 and ERK1 and no detectable binding to the other 11 MAPKs.

An Intact FRIEDE Motif Is Essential for Both ERK3 and ERK4 to Mediate Both Cytoplasmic Translocation and Activation of MK5—To assess the validity of these data *in vivo*, a selection of the point mutations that affected binding to MK5 were introduced into the FRIEDE motif of full-length ERK4. ERK4 F328A, ERK4 F328Y, ERK4 I330K, and ERK4 F328A were assayed for binding to EGFP-MK5 in series of co-immunoprecipitation experiments following co-expression in HeLa cells. In agreement with the peptide array data, ERK4 carrying the F328A mutation displayed a much reduced ability to bind to MK5, whereas the effect of the ERK4 F328Y substitution was somewhat intermediate (Fig. 4*A*). In contrast to F328A and F328Y, substitution of isoleucine 1330 for lysine (ERK4 I330K) completely abrogated binding to EGFPMK5 as well as to endogenous MK5 (Fig. 4, *A* and *C*, respectively). We also changed the corresponding isoleucine in ERK3 (Ile^{334}) to lysine by site-directed mutagenesis, and as depicted in Fig. 4*B* this ERK3 mutant was also unable to interact with MK5.

ERK3 is a highly unstable protein with a half-life of 30–45 min in exponentially proliferating cells (10). Down-regulation of MK5 expression either by small interfering RNA-mediated knockdown or its elimination by gene knock-out leads to a dramatic reduction in ERK3 protein levels (11, 33). Conversely, the reintroduction of MK5 into either knock-out or knockdown cells rescued the ERK3 protein level, suggesting that MK5 acts as a chaperone for ERK3. To investigate whether MK5 could stabilize a mutant of ERK3 that was unable to bind MK5, we

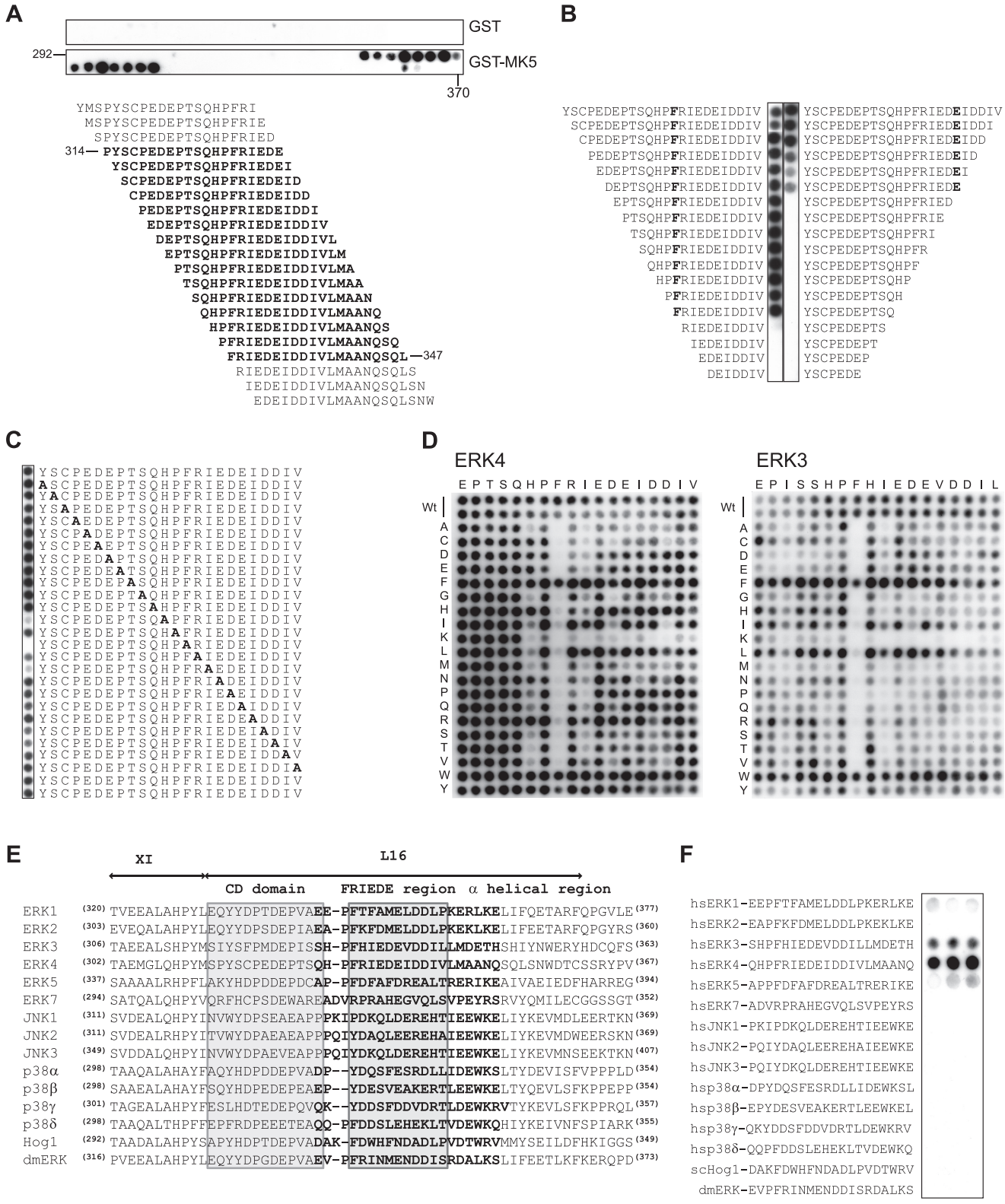

FIGURE 3. **Identification of the FRIEDE motif within the L16 loop of ERK4 as an MK5 binding determinant.** In all overlay assays, the indicated peptide sequences were bound on cellulose membranes and probed with 1 μg/ml GST or GST-MK5 for 2 h and detected with an anti-GST antibody conjugated to horseradish peroxidase. Overlay assay with GST alone gave little or no signal in all experiments (*A* and data not shown). *A*, a sequence corresponding to amino acids 292–370 was spotted as 20-mer peptides on a cellulose filter as a 1-amino acid shifted array covering the entire sequence. Positive spots correspond to the highlighted sequences. *B*, increasing N- and C-terminal truncations of the ERK4 sequence were spotted and evaluated for MK-5 binding. Amino acids defining the binding boundaries are *highlighted*. *C*, the ERK4 sequence was subjected to an alanine scan by sequential substitution to identify critical amino acids for binding to MK-5. *D*, a two-dimensional peptide array was constructed by replacing the 18-residue sequence in ERK4 (*left panel*) and the homologous region of ERK3 (*right panel*) with all 20 amino acids as indicated. *E*, alignment of the kinase domain XI and L16 including the CD domain and the FRIEDE motif for the indicated MAPKs is shown. *F*, to test the specificity of MK5 for the FRIEDE motif in ERK3 and ERK4, we spotted the corresponding sequences of the indicated MAPKs in triplicates on a filter and probed with GST-MK5.

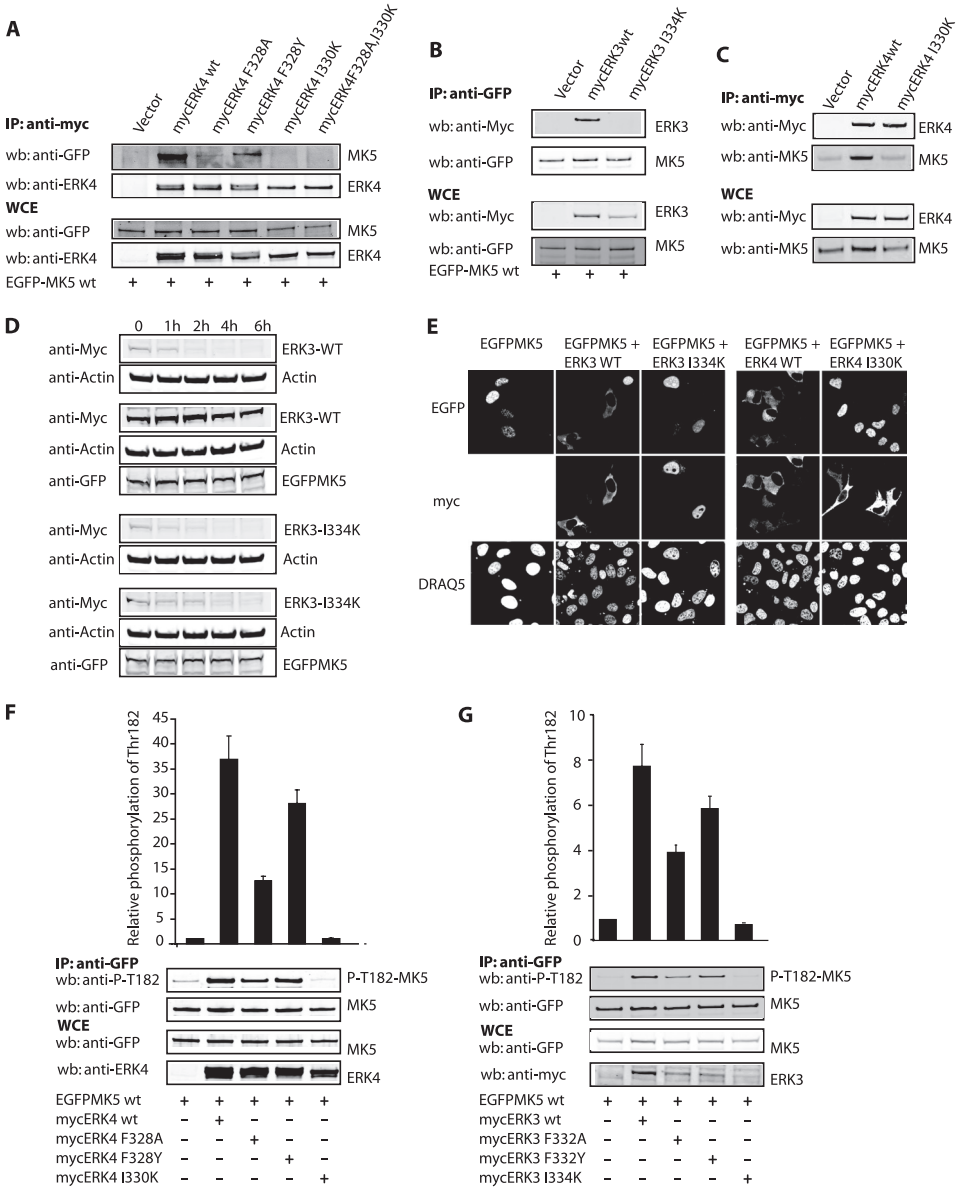

FIGURE 4. **Mutations in the FRIEDE motif affect the ability of both ERK3 and ERK4 to interact with, translocate, and activate MK5.** *A*, HeLa cells were transfected with the indicated versions of Myc-tagged ERK4 and WT EGFP-MK5. After 24 h, the cells were lysed, and Myc-ERK4 was immunoprecipitated (*IP*) using an anti-Myc antibody. The immunoprecipitates were analyzed by SDS-PAGE and Western blotting (*wb*) using an anti-GFP antibody for MK5 (*top panel*), an anti-ERK4 antibody for ERK4 (*second panel*). *B*, HeLa cells were co-transfected with vectors encoding Myc-ERK3 WT or Myc-ERK3 I334K and EGFP-MK5 WT. After 24 h, whole cell extracts were prepared, and EGFP-MK5 was immunoprecipitated with an anti-GFP antibody. ERK3 and EGFP-MK5 were detected by Western blotting using an anti-Myc antibody or a polyclonal anti-GFP antibody, respectively. *C*, HeLa cells were transfected with the indicated vectors. After 24 h, whole cell extracts were prepared, and Myc-tagged ERK4 was immunoprecipitated with an EZview anti c-Myc affinity gel. The immunoprecipitates were then analyzed by SDS-PAGE and Western blotting using an anti-Myc antibody to detect ERK4 and a monoclonal antibody against MK5. *D*, HeLa cells were transfected with Myc-ERK3-WT or Myc-ERK3 I334K alone or together with EGFP-MK5 WT. After 24 h, cycloheximide (10 μg/ml) was added, and the cells were harvested at the indicated time. ERK3 were visualized by Western blotting using an anti-Myc antibody. The blots were also probed with anti-actin antibody to ensure equal loading and anti-GFP antibody to verify expression of EGFP-MK5. *E*, HeLa cells were transfected with expression vectors encoding either EGFP-MK5 alone or in combination with either Myc-ERK3 WT, Myc-ERK3 I334K Myc-ERK4 WT, and Myc-ERK4 I330K. After 24 h the cells were fixed, and EGFP-MK5 was visualized directly (*top panel*). ERK3 and ERK4 were visualized by staining with an anti-Myc antibody and Alexa 594 anti-mouse antibody (*middle panel*). The nuclei were visualized by DRAQ5 staining (*bottom panel*). *F* and *G*, HeLa cells were co-transfected with the indicated expression plasmids encoding the indicated versions of Myc-tagged ERK3 (*G*) or Myc-tagged ERK4 (*F*) and EGFP-tagged MK5. After 24 h, the cells were lysed, and EGFP-MK5 was immunoprecipitated using an anti-GFP antibody. The immunoprecipitates were analyzed by SDS-PAGE and Western blotting using a phospho-specific antibody raised against Thr^{182} of MK5 (*top panel*), and an anti-GFP antibody for EGFPMK5 (*second panel*). The data in *E* and *F* and two similar experiments were quantified using the Odyssey infrared imaging system. The relative intensity of the bands are shown using the band from single transfected EGFP-MK5 as 1 with S.E. Expression of MK5 and wild type and mutant forms of ERK3 and ERK4 was verified by Western blotting of cell lysates (*WCE*) using appropriate antibodies (*bottom panels* in *A–C*, *F*, and *G*).

expressed WT or I334K mutant of ERK3 with and without MK5 in the presence of cycloheximide. Extracts from transfected cells were harvested at different time points after the addition of cycloheximide, and the rate of ERK3 degradation was monitored by Western blotting. In agreement with earlier studies, ERK3 was unstable showing significant turnover within 2 h of cycloheximide addition (Fig. 4*C*). Co-expression of MK5 resulted in significant stabilization of WT ERK3 but had little or no effect on the stability of ERK3 I334K (Fig. 4*C*).

We have previously demonstrated that a deletion mutant of either ERK3 or ERK4 lacking the FRIEDE region failed to either interact with or to activate MK5 (9). Thus, the activation of MK5 by either ERK3 or ERK4 is absolutely dependent on specific interactions between these proteins. Furthermore, we previously demonstrated that the activation of MK5 required ERK3- or ERK4-mediated phosphorylation of Thr^{182} within the activation loop of MK5 (9). Using Thr^{182} phosphorylation to monitor MK5 activity, we asked whether the reduced ability of the ERK3 and ERK4 FRIEDE mutants to bind to MK5 was accompanied by a reduced ability to activate MK5 *in vivo*. To this end we co-transfected wild type MK5 with either of the ERK3 or ERK4 FRIEDE mutants in HeLa cells. MK5 was then immunoprecipitated from the extracts and immunoblotted using a phospho-specific antibody raised against Thr^{182}. A strict correlation between binding affinity and levels of MK5 Thr^{182} phosphorylation was observed. Expression of either wild type or the F332Y or F328Y mutants of ERK3 and ERK4, respectively, both of which bind to MK5, increased levels of Thr^{182} phosphorylation by severalfold. ERK3 F332A or ERK4 F328A, which bind to MK5 with a lower affinity, displayed a reduced ability to phosphorylate wild type MK5, whereas ERK3 I334K or ERK4 I330K, both of which

are unable to interact with MK5, failed to increase levels of Thr[182] phosphorylation.

DISCUSSION

In this study we have defined and functionally characterized the interaction between ERK3/4 and MK5. The specificity of interactions between classical MAPKs and their respective MAPKAPKs are known to be mediated through the conserved CD domain in the MAPKs, which recognize specific D motifs found in the MAPKAPKs. The negatively charged CD domain is conserved in both ERK3 and ERK4, and MK5 also possesses a functional D motif (35). However, previously published data suggest that these determinants are not involved in the interaction between ERK3/4 and MK5 (9, 11, 26, 33). The results we have obtained in the present study using mutants within the CD domains of both ERK3 and ERK4 support this conclusion. The ED domain constitutes an additional cluster of negatively charged residues important for the interaction between MAPKs and MAPKAP kinases (20). This is situated in the docking groove close to the CD domain in the tertiary structure of the MAPKs (20). Mutation of two characteristic residues within this motif of ERK3 or ERK4 did not affect complex formation with MK5. Thus, neither the CD domain nor the ED site of ERK3 and ERK4 seem to be involved in the interaction with their downstream target MK5. This begs the question as to why the CD domain is so highly conserved in ERK3 and ERK4? The answer is likely to be that it is important in mediating specific binding to other ERK3/ERK4 binding partners, and we have preliminary data to suggest that this may indeed be the case.[3]

We defined the minimal domain in the C terminus of MK5 involved in the specific binding to ERK3 and ERK4. Although removal of as little as 13 residues from the C terminus of MK5 disrupts the interaction with ERK4, this 13-residue peptide is not sufficient for interaction with MK5. The inability of short peptide motifs from MK5 to mediate ERK3/4 interaction is also supported by our experiments using the peptide overlay method where we were unable to detect any 20-mer peptides from MK5 that could mediate interaction with either ERK4 or ERK3 (data not shown). This contrasts with reports describing other MAPK MAPKAPK interactions in which short D motif peptides as small as 16 residues are sufficient for interaction (36). The minimal domain of MK5 required for the interaction with ERK4 turned out to be the whole C-terminal extension of MK5. This extension is unique to MK5 and is not found in MK2 and MK3 and may explain the specificity of MK5 for ERK3 and ERK4. Data from the C-terminal deletion mutants of MK5 suggest that several binding determinants reside in this region. Individually they are insufficient for interaction, but together they are able to mediate tight and stable interaction with both ERK3 and ERK4.

By the use of a peptide array, we identified a minimal motif in ERK4 ([328]FRIEDEIDD[336]) responsible for interaction with MK5. A two-dimensional peptide scan in which the residues in every position in the interacting peptide was changed to each of the residues in the basic set of 20 amino acids revealed that only amino acids carrying aromatic side chain were accepted in position 328 of ERK4 (position 332 in ERK3). Lysine was not tolerated in any position within the region comprising residues His[326] to Val[338] (His[330] to Leu[342] for ERK3).

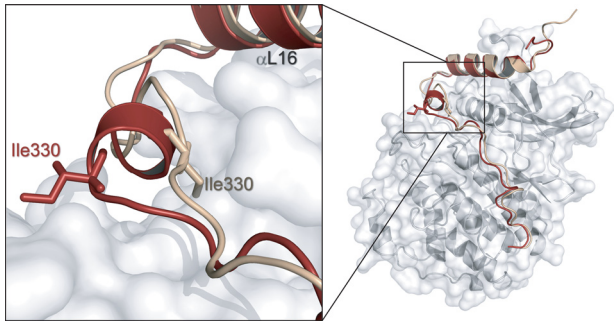

FIGURE 5. **Molecular modeling reveals that activation loop phosphorylation of ERK4 most likely results in a greater exposure of Ile[330] to solvent.** ERK4 residues 1–359 were modeled using unphosphorylated ERK2 and dually phosphorylated (activated) ERK2 as templates. The L16 C-terminal extension of unphosphorylated (*beige*) and phosphorylated ERK4 (*red*) are shown, and the critical isoleucine 330 residue is *highlighted*.

Several earlier studies have proposed that this part of the L16 loop of MAPKs may be a protein-protein interaction motif involved in homodimerization (29, 37). However, this study is the first to demonstrate that a MAPK uses this region for binding to another protein. One important characteristic of the interaction between both ERK3 and ERK4 and MK5 is that the protein-protein interaction mediated by the FRIEDE motif is absolutely dependent on phosphorylation of the SEG motif within the activation loop of these atypical MAPKs (27, 28). This implies that activation loop phosphorylation may alter or expose the L16 region of ERK3 and ERK4 containing the FRIEDE motif, thus facilitating its interaction with MK5.

Some clues as to how this might occur come from studies of the corresponding domains in the classical MAPK ERK2. This phosphorylation-dependent movement in the critical residues in the FRIEDE motif can be modeled using the crystal structures of unphosphorylated and phosphorylated ERK2 (Fig. 5). This model strongly suggests a molecular relationship between the phosphorylation status of the activation loop and the binding of downstream effectors to the FRIEDE motif within ERK3 and ERK4. In the unphosphorylated (inactive) conformation, the critical Ile[330] residue is buried against the αC helix. However, phosphorylation of the activation loop leads to a conformational change in the region of the FRIEDE motif, which results in the surface exposure of Ile[330] and may facilitate its participation in protein-protein interactions with MK5.

In ERK2, the L16 region of ERK2 is important for mediating the phosphorylation-dependent homodimerization of this MAPK (38). Dual phosphorylation of the T*X*Y motif induces conformational changes in the activation loop. This in turn leads to altered interaction with key structural elements including L16, with this latter change resulting in exposure of the dimerization interface. Phe[329], the residue corresponding to Ile[330] of ERK4, flips to the surface where it is important for dimerization through a stacking interaction between its aromatic ring and His[176] of the activation loop.

Despite the fact that the activation loops of both ERK3 and ERK4 are identical in length to that found in ERK2, these atypical MAPKs also lack key conserved residues found in ERK2

[3] M. Perander, S. M. Keyse, and O. M. Seternes, unpublished observations.

that mediate dimerization. In support of this we have been unable to demonstrate the existence of either ERK3/ERK4 homo- or heterodimers in our experimental systems (data not shown). Another important difference between the mode of binding between ERK3/ERK4 and MK5 and formation of ERK2 dimers is that a single amino acid substitution within the FRIEDE motif (Ile^{334} in ERK3 and Ile^{330} in ERK4 to lysine) is sufficient to block MK5 binding. In contrast, single or even quadruple amino acid changes were not sufficient to abrogate ERK2 dimerization (38). This required either the introduction of a charge repulsion (H176E) or deletion of residues from the ERK2 activation loop (Pro^{174}–Asp^{177}) (38, 39).

Although dual phosphorylation of ERK2 leads to profound changes in L16, binding of peptides or modification of this region may also influence the structure of the activation loop as well. Interestingly Salvador *et al.* (40) have recently shown that Tyr^{323} of p38 MAPK, which corresponds to Phe^{328} of ERK4, is a novel phosphorylation site. Phosphorylation of this site by ZAP-70 in activated T-cells results in autophosphorylation and subsequent activation of p38 MAPK. Moreover, Diskin *et al.* (41) were able to develop intrinsically active kinases by mutagenesis of p38 MAPK in the region corresponding to the FRIEDE motif of ERK4. Crystal structures of these mutants revealed that local alternations in the L16 loop region promote kinase activation (37). Based on these structures the authors propose that the L16 may function as a molecular switch that upon conformational alternation promotes activation.

Taken overall, these observations imply there is a high level of two-way communication between the activation loop of the MAPKs and the L16 region, which contains the FRIEDE motif in both ERK3 and ERK4. Conformational change within this region following activation loop phosphorylation may promote binding to MK5 as depicted in Fig. 5. Conversely, the increase of ERK4 Ser^{186} phosphorylation, which was observed previously after MK5 binding and which occurred independently of MK5 kinase activity, could be due to changes in the activation loop induced by MK5 binding to the FRIEDE region (27, 28). This change could then either make the Ser^{186} inaccessible to a protein phosphatase or make it more accessible to the putative ERK3/4 kinase.

In conclusion we have shown that both ERK3 and ERK4 do not use the classical CD domain and cognate D motif to bind to and activate their downstream substrate MK5. Instead we have demonstrated that a novel MAPK docking site termed the FRIEDE motif that is located in the L16 loop of ERK4 C-terminal to the CD domain is required for interaction with the unique C-terminal extension of MK5. Structural data from the corresponding region in ERK2 suggest that this region undergoes substantial changes upon phosphorylation of the activation loop (29) and suggest a molecular relationship between activation loop status and binding of downstream effectors to the FRIEDE motif. Future work will be directed toward structural and biochemical studies of the ERK3/4 domain containing this motif and its ability to bind to MK5. The identification of this conserved region may also facilitate the discovery of other interacting partners and regulators of ERK3 and ERK4 *in vivo* and the physiological consequences of complex formation between these two signaling proteins and MK5.

Acknowledgments—We thank Prof. Philip Cohen and the protein production and antibody purification teams (Division of Signal Transduction Therapy, University of Dundee) co-coordinated by Hilary McLauchlan and James Hastie and Prof. Terje Johansen (University of Tromsoe) for antibodies.

REFERENCES

1. Raman, M., Chen, W., and Cobb, M. H. (2007) *Oncogene* **26,** 3100–3112
2. Avruch, J. (2007) *Biochim. Biophys. Acta* **1773,** 1150–1160
3. Bogoyevitch, M. A., and Court, N. W. (2004) *Cell Signal.* **16,** 1345–1354
4. Roux, P. P., and Blenis, J. (2004) *Microbiol. Mol. Biol. Rev.* **68,** 320–344
5. Turjanski, A. G., Vaqué, J. P., and Gutkind, J. S. (2007) *Oncogene* **26,** 3240–3253
6. Qi, M., and Elion, E. A. (2005) *J. Cell Sci.* **118,** 3569–3572
7. Cuenda, A., and Rousseau, S. (2007) *Biochim. Biophys. Acta* **1773,** 1358–1375
8. Kostich, M., English, J., Madison, V., Gheyas, F., Wang, L., Qiu, P., Greene, J., and Laz, T. M. (2002) *Genome Biol.* **3,** RESEARCH0043
9. Aberg, E., Perander, M., Johansen, B., Julien, C., Meloche, S., Keyse, S. M., and Seternes, O. M. (2006) *J. Biol. Chem.* **281,** 35499–35510
10. Coulombe, P., Rodier, G., Pelletier, S., Pellerin, J., and Meloche, S. (2003) *Mol. Cell. Biol.* **23,** 4542–4558
11. Seternes, O. M., Mikalsen, T., Johansen, B., Michaelsen, E., Armstrong, C. G., Morrice, N. A., Turgeon, B., Meloche, S., Moens, U., and Keyse, S. M. (2004) *EMBO J.* **23,** 4780–4791
12. Gaestel, M. (2006) *Nat. Rev. Mol. Cell Biol.* **7,** 120–130
13. Ranganathan, A., Pearson, G. W., Chrestensen, C. A., Sturgill, T. W., and Cobb, M. H. (2006) *Arch. Biochem. Biophys.* **449,** 8–16
14. Goldsmith, E. J., Akella, R., Min, X., Zhou, T., and Humphreys, J. M. (2007) *Chem. Rev.* **107,** 5065–5081
15. Sharrocks, A. D., Yang, S. H., and Galanis, A. (2000) *Trends Biochem. Sci.* **25,** 448–453
16. Tanoue, T., and Nishida, E. (2003) *Cell Signal.* **15,** 455–462
17. Mooney, L. M., and Whitmarsh, A. J. (2004) *J. Biol. Chem.* **279,** 11843–11852
18. Bhattacharyya, R. P., Reményi, A., Yeh, B. J., and Lim, W. A. (2006) *Annu. Rev. Biochem.* **75,** 655–680
19. Tanoue, T., Adachi, M., Moriguchi, T., and Nishida, E. (2000) *Nat. Cell Biol.* **2,** 110–116
20. Tanoue, T., Maeda, R., Adachi, M., and Nishida, E. (2001) *EMBO J.* **20,** 466–479
21. Chang, C. I., Xu, B. E., Akella, R., Cobb, M. H., and Goldsmith, E. J. (2002) *Mol. Cell* **9,** 1241–1249
22. Zhang, J., Zhou, B., Zheng, C. F., and Zhang, Z. Y. (2003) *J. Biol. Chem.* **278,** 29901–29912
23. Kallunki, T., Su, B., Tsigelny, I., Sluss, H. K., Dérijard, B., Moore, G., Davis, R., and Karin, M. (1994) *Genes Dev.* **8,** 2996–3007
24. Robinson, F. L., Whitehurst, A. W., Raman, M., and Cobb, M. H. (2002) *J. Biol. Chem.* **277,** 14844–14852
25. Xu, B., Stippec, S., Robinson, F. L., and Cobb, M. H. (2001) *J. Biol. Chem.* **276,** 26509–26515
26. Kant, S., Schumacher, S., Singh, M. K., Kispert, A., Kotlyarov, A., and Gaestel, M. (2006) *J. Biol. Chem.* **281,** 35511–35519
27. Déléris, P., Rousseau, J., Coulombe, P., Rodier, G., Tanguay, P. L., and Meloche, S. (2008) *J. Cell. Physiol.* **217,** 778–788
28. Perander, M., Aberg, E., Johansen, B., Dreyer, B., Guldvik, I. J., Outzen, H., Keyse, S. M., and Seternes, O. M. (2008) *Biochem. J.* **411,** 613–622
29. Canagarajah, B. J., Khokhlatchev, A., Cobb, M. H., and Goldsmith, E. J. (1997) *Cell* **90,** 859–869
30. Lamark, T., Perander, M., Outzen, H., Kristiansen, K., Øvervatn, A., Michaelsen, E., Bjørkøy, G., and Johansen, T. (2003) *J. Biol. Chem.* **278,** 34568–34581
31. Kramer, A., and Schneider-Mergener, J. (1998) *Methods Mol. Biol.* **87,** 25–39
32. Guex, N., and Peitsch, M. C. (1997) *Electrophoresis* **18,** 2714–2723
33. Schumacher, S., Laass, K., Kant, S., Shi, Y., Visel, A., Gruber, A. D.,

Kotlyarov, A., and Gaestel, M. (2004) *EMBO J.* **23,** 4770–4779
34. Brunner, D., Oellers, N., Szabad, J., Biggs, W. H., 3rd, Zipursky, S. L., and Hafen, E. (1994) *Cell* **76,** 875–888
35. Seternes, O. M., Johansen, B., Hegge, B., Johannessen, M., Keyse, S. M., and Moens, U. (2002) *Mol. Cell. Biol.* **22,** 6931–6945
36. Smith, J. A., Poteet-Smith, C. E., Lannigan, D. A., Freed, T. A., Zoltoski, A. J., and Sturgill, T. W. (2000) *J. Biol. Chem.* **275,** 31588–31593
37. Diskin, R., Lebendiker, M., Engelberg, D., and Livnah, O. (2007) *J. Mol. Biol.* **365,** 66–76
38. Khokhlatchev, A. V., Canagarajah, B., Wilsbacher, J., Robinson, M., Atkinson, M., Goldsmith, E., and Cobb, M. H. (1998) *Cell* **93,** 605–615
39. Wilsbacher, J. L., Juang, Y. C., Khokhlatchev, A. V., Gallagher, E., Binns, D., Goldsmith, E. J., and Cobb, M. H. (2006) *Biochemistry* **45,** 13175–13182
40. Salvador, J. M., Mittelstadt, P. R., Guszczynski, T., Copeland, T. D., Yamaguchi, H., Appella, E., Fornace, A. J., Jr., and Ashwell, J. D. (2005) *Nat. Immunol.* **6,** 390–395
41. Diskin, R., Askari, N., Capone, R., Engelberg, D., and Livnah, O. (2004) *J. Biol. Chem.* **279,** 47040–47049